Kinetics of Cl Atom Reactions with Methane, Ethane, and Propane from 292 to 800 K

Jeffrey S. Pilgrim,[†] Andrew McIlroy,[†,‡] and Craig A. Taatjes*

Combustion Research Facility, Mail Stop 9055, Sandia National Laboratories, Livermore, California 94551-0969

Received: September 23, 1996; In Final Form: January 3, 1997[⊗]

Absolute rate coefficients for the reactions of chlorine atom with methane and ethane between 292 and 800 K and with propane between 292 and 700 K have been determined using the laser photolysis/continuous wave infrared long-path absorption method, LP/cwIRLPA. A novel reactor design and optical arrangement allow long absorption paths with precise control of the temperature in the probed volume. The rate coefficient for methane exhibits significant curvature between 292 and 800 K and can be described over this temperature range by a modified Arrhenius expression, $k_{CH_4}(T) = [3.7(^{+8.2}_{-2.5}) \times 10^{-13}$ cm^3 molecule^{-1} s$^{-1}](T/298)^{2.6(\pm0.7)}$ exp$[-385(\pm320)/T]$ (all error bars are $\pm2\sigma$ precision only). In the temperature range 292−600 K the rate with ethane agrees well with earlier investigations, fitting a simple Arrhenius expression $k_{C_2H_6}(T) = 8.6(\pm0.5) \times 10^{-11}$ exp$[-135(\pm26)/T]$ cm^3 molecule^{-1} s^{-1}. However, as the temperature increases beyond 600 K the Arrhenius plot exhibits significant upward curvature. Over the range 292−800 K a three-parameter Arrhenius fit, $k_{C_2H_6}(T) = 3.4(\pm1.4) \times 10^{-11}(T/298)^{0.7(\pm0.3)}$ exp$[150(\pm110)/T]$ cm^3 molecule^{-1} s^{-1}, models the experimental data adequately. The rate coefficient for propane is found to be independent of temperature and equal to $1.38(\pm0.03) \times 10^{-10}$ cm^3 molecule^{-1} s^{-1}.

Introduction

The role of Cl atom in stratospheric ozone depletion has led to extensive investigation of its reactivity with atmospheric species over the past several decades. Cl atom destruction of the ozone layer proceeds catalytically and would continue unchecked if it were not for competing reactions such as those with small alkanes, of which methane is the most abundant atmospherically. The Cl atom reaction also represents a significant loss channel for stratospheric methane, which impacts greenhouse gas models. As a result, there have been many kinetic studies of the reaction of Cl with methane and ethane over the temperature range relevant to atmospheric chemistry.[1−5] Another area where Cl reactions are important is the incineration of current chlorofluorocarbons (CFC) and chemical weapons stockpiles. Cl atoms are also generated during the combustion of chlorinated plastics. In addition, chlorine-containing contaminants in more standard combustion systems, such as biomass, coal, black liquor, and waste incineration, are responsible for the production of toxic chlorinated organic species. Incineration of these species generates free Cl atoms that can then react with excess fuel. Kinetic information for these reactions at elevated temperatures is needed for modeling combustion processes. Since the Cl + CH_4 and Cl + C_2H_6 reactions are also widely used as reference reactions in relative rate studies, highly accurate reference rate coefficients are critical.[6,7] High-quality Arrhenius parameters for these reference reactions facilitate temperature-dependent relative rate determinations. Additionally, the extent of deviation from simple Arrhenius behavior is important for ascertaining reaction mechanisms, as well as for increasing the reliability of parametrized data for use in reaction system modeling. In the present work we report measurements of Cl atom reaction kinetics with methane and ethane between 292 and 800 K and with propane between 292 and 700 K.

Absolute rate coefficients are obtained in a slow flow reactor using pulsed laser photolysis with continuous wave infrared laser detection of the HCl reaction product. A novel multipass optical arrangement allows precise control of the pump−probe overlap and provides several meters of usable path length while avoiding contributions to the signal from the cooler regions of the reaction cell. This arrangement may be expected to yield more accurate results than a line-of-sight measurement, especially for strongly temperature-dependent reactions.

The present study extends the previous high-temperature limits for these three reactions and provides precise measurements of the temperature dependence. In the methane system significant curvature is seen in an Arrhenius plot, in qualitative agreement with the predictions of simple transition-state theory calculations. The ethane system also displays a marked deviation from simple Arrhenius behavior above 600 K. However, the reaction with propane is found to have no temperature dependence over the range 292−700 K.

Experimental Section

Technique. Absolute reaction rates of the chlorine + hydrocarbon systems are investigated using the laser photolysis/continuous wave infrared long-path absorption, LP/cwIRLPA, method.[8−10] Chlorine atoms are generated from photolytic precursors by a pulsed excimer laser, and the subsequent time evolution of the HCl reaction product is monitored by absorption of a continuous wave (CW) infrared beam. Using a CW probe beam allows the full time profile of the reaction to be obtained for each photolysis laser shot. Signal averaging is then employed to improve signal-to-noise ratios.

The rise time of the detector used to monitor the IR absorption and diffusion of the probed species out of the viewing region limits the kinetic time constants that can be studied in the LP/cwIRLPA reactor. The rise time of the InSb detectors used in these experiments is around 50 ns, but the instrument response is limited by the preamplifier rise time of 200 ns. The diffusion time scale for HCl at the 10 Torr pressure of these experiments is well over 10 ms. Kinetic time constants in the range of 1 μs

[†] Sandia National Laboratories Postdoctoral Research Associate.
[‡] Present address: M5/754, The Aerospace Corporation, PO Box 92457, Los Angeles, CA 90009-2457.
* Author to whom correspondence should be addressed.
[⊗] Abstract published in *Advance ACS Abstracts,* February 15, 1997.

S1089-5639(96)02916-7 CCC: $14.00

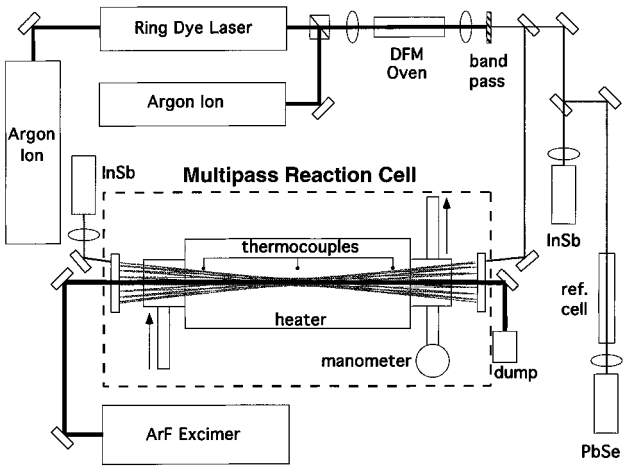

Figure 1. Schematic of the laser photolysis/infrared long-path absorption apparatus. The infrared beam from difference frequency mixing of a CW ring laser and Ar ion laser is incorporated into a Herriott-type multipass cell. This system consists of nine passes with an effective path length of over 3 m. Adjusting the diameter of the photolysis laser constrains the overlap to the center of the cell where the temperature is flat and stable. A reference cell is used to tune the infrared beam to the R(3) fundamental transition of the HCl reaction product.

to 1 ms can be accurately determined in the present system; in this study all pseudo-first-order decays are at least 10 times the detector rise time, which results in an accurate representation of the temporal evolution of the reaction. Losses due to diffusion are 2−3 orders of magnitude smaller than the pseudo-first-order rate constants in all experiments.

The effects of secondary reactions of Cl atoms with reaction products, e.g., with ethane produced by recombination of methyl radicals from Cl + methane, are minimized by operating the reactor under conditions where the reactant mixture is replenished between photolysis pulses. In the present study, this requirement constrains the photolysis laser repetition rate to around 2 Hz for typical flow conditions. The measured rate coefficients are constant while the photolysis laser pulse energy and photolyte concentration are varied by factors of 5, confirming that both side reactions with radicals produced in the photolysis and secondary reactions of alkyl radicals products are insignificant in the present experiments.

Reactor. The flow reactor employed in the present study is a stainless steel cylinder 1 m long and 50 mm in diameter. Both ends are sealed using Brewster angle windows of CaF_2 13 mm thick. Figure 1 is a schematic of the experimental setup. The chlorine photolytic precursor, hydrocarbon reactant, and buffer gas enter the reactor through a side-arm on the upstream end from separate calibrated mass flow controllers. Pure CF_2Cl_2 (99.9%) is used as the photolyte, and the buffer gas is Ar (99.9995%). The pressure in the cell is actively controlled by a throttle valve and a mechanical vacuum pump and monitored by a capacitance manometer. For a given total flow, the throttle valve is opened or closed under feedback from the capacitance manometer to maintain the desired pressure.

Surrounding the flow reactor's 60 cm long midsection is a commercial ceramic-fiber heater capable of reaching temperatures in excess of 1200 K. However, the temperature profile across this heater is not uniform, with a steep temperature gradient near the edges of the heater. To counteract the heat loss at the ends of the cell/heater unit, separate homemade nichrome wire heaters were installed on both ends, consisting of several turns of wire covered with ceramic insulator beads to evenly distribute the heat as well as for electrical insulation from the stainless steel cell body. These heaters serve to balance the thermal load from heat leakage to the ambient surroundings, thus extending the flat temperature profile. Three independent chromel/alumel, K-type thermocouples are located inside the flow reactor body. Each thermocouple is connected to a microprocessor-based temperature controller, and each controller has independent control of one of the three heaters. One thermocouple in the center of the cell is used to provide the temperature feedback for the fiber heater. The other two thermocouples, placed just inside the nichrome heater winding locations, control the end heaters. The usable uniform temperature region with the three heater/three controller system is ∼35 cm in the flow cell midsection. The temperature variation over this region is approximately ±2 K at 800 K.

IR Generation and Multipass Cell. The tunable CW infrared radiation for these experiments is generated by difference frequency mixing, DFM, in temperature-tuned $LiNbO_3$ after a design pioneered by Pine.[11] The pump laser is a single frequency argon ion laser operating on the 514.5 nm line. Tunable signal laser radiation comes from a ring dye laser operating on rhodamine 6G around 607 nm. These lasers are rendered collinear and sent into the 4 mm × 4 mm × 50 mm $LiNbO_3$ crystal inside a temperature-controlled oven. The oven is heated to the necessary temperature to provide correct phase-matching for maximum IR generation. Typical input powers are 500 and 600 mW for the argon ion and dye laser, respectively. Approximately 6 μW of tunable IR power at 3.3 μm is obtained with proper focusing of the input beams.

A band-pass filter blocks the residual input laser beams while passing the IR beam. This beam is then split into approximately equal signal and reference beams. The reference beam is subsequently split again with part of the beam going through an HCl reference cell and onto a PbSe detector. The other part of the reference beam goes through an IR polarizer and band-pass filter and, finally, onto an InSb detector. The power on the reference detector is controlled by the orientation of the IR polarizer.

In the experiments described here, a Herriott-type multipass arrangement is employed to increase the detection sensitivity.[12−14] This particular arrangement is especially well-suited to the present application. The Herriott cell uses off-axis paths in a spherical resonator, which causes the traversing beam to trace out a circle of spots on each mirror. However, the beam never crosses the center of the cell. Instead the beam path maps out a smaller circle in the center of the cell (for identical end mirrors) whose dimensions are readily calculable. In the present experiments the beams are coupled in and out through uncoated sections of the spherical mirrors. The pump beam propagates through the uncoated center of each optic and travels down the resonator axis. The pump−probe overlap region is therefore confined to the center of the cell in the region where the diameter of the circle defined by the probe beam path is smaller than the diameter of the pump beam. This is in contrast to, for example, a White cell where the beams cross the center of the cell and probe the entire volume between the end mirrors.

In fact, it is not desirable to probe the entire cell volume in these kinetics experiments. There is a temperature gradient established between the 30−35 cm of controlled temperature region in the cell midsection and the cell ends that are exposed to ambient conditions. Thus, a line-of-sight measurement down the cell axis or a White-type multipass arrangement that probes the whole cell volume will contain spurious kinetic information from these uncharacterized temperature regions. In the Herriott arrangement, on the other hand, the photolysis laser beam diameter can be adjusted so that the overlap with the IR beam is confined to the interior of the reaction cell with an adjustable and well-quantified linear extent. For the experiments described

here, the multipass cell consists of nine passes with an effective probe length of more than 3 m. Although this is not an extremely large path length, it is confined to a well-characterized temperature region. In addition, this system has been recently redesigned and upgraded to 31 passes, which gives an effective usable path length of over 12 m.[14]

After traversing the multipass cell, the IR signal beam goes through a band-pass filter and is focused onto an InSb signal detector. The signal from this detector and the signal from the reference detector are then amplified 50× and subtracted in a differential preamplifier. Subtraction of these matched detectors reduces the effects of laser amplitude noise. The difference signal is zeroed with the IR polarizer in the reference beam path prior to taking data so that differential absorption is caused only by the product HCl in the flow cell. To aid in tuning the IR wavelength to the correct HCl transition, absorption of the split and chopped signals through the reference cell is monitored while the ring dye frequency is tuned. The R(3) line of the $H^{35}Cl$ fundamental vibrational transition is used for absorption because of the high thermal population in $J = 3$. Rotational relaxation will be rapid compared to the reaction rates,[15] even for high rotational states,[16] and the reactions are not sufficiently exothermic to produce vibrationally excited HCl, ensuring that the absorption signal is a faithful representation of the HCl population. Signal from the preamplifier is fed into a digital storage oscilloscope where it is digitized and averaged. The resulting time trace is transferred to a microcomputer for storage and analysis.

Specific Kinetic Conditions. Chlorine atoms are generated from the 193 nm photolysis of CF_2Cl_2. The 193 nm beam is generated by an excimer laser operating on ArF. Fluence at the cell is kept around 5−10 mJ pulse^{-1} cm^{-2}. At 193 nm the principal dissociation process yields one chlorine atom while about 30% of the photons absorbed yield two chlorine atoms.[17] The absorption at 193 nm is kept below a few percent to provide a uniform chlorine atom concentration across the reaction cell. The concentration of the photolyte (3×10^{14} molecules cm^{-3}) guarantees that the concentration of generated chlorine atoms is much less than that of the hydrocarbon reagent, keeping the kinetics in the pseudo-first order limit. In addition, the reaction conditions are selected so that absorption by the HCl product is kept below 5% and in the linear regime.

The total pressure in the reaction cell was normally held at 10 Torr with a total gas flow rate of about 900 sccm (standard cubic centimeter per minute). At this pressure, thermal equilibration of the photolytically produced Cl atoms and the HCl reaction product is rapid relative to the kinetic time scale. In a typical run, the hydrocarbon concentration is varied over a factor of 7 or 8 (5×10^{14} to 3×10^{15} molecules cm^{-3}). Figure 2 shows a typical time trace of the absorption profile for the HCl product from the Cl + propane reaction. In these systems, the production of HCl has the same time behavior as the loss of Cl. Since $[HCl]_t = [Cl]_0 - [Cl]_t$ from mass balance, $[HCl]_t$ is given by

$$[HCl]_t = [Cl]_0(1 - e^{-k_1[C_nH_{2n+2}]t}) \qquad (1)$$

The measured HCl time traces are fitted using the functional form of eq 1 to extract $k_1[C_nH_{2n+2}]$, where $[C_nH_{2n+2}]$ is known from the flow conditions and is essentially constant. This pseudo-first-order time constant is measured as a function of $[C_nH_{2n+2}]$, and the second-order rate coefficient for the reaction, k_1, is extracted as the slope of a plot of pseudo-first-order rate coefficients vs alkane concentration. A typical plot for each of the three reactants is shown in Figure 3. Nonzero intercepts

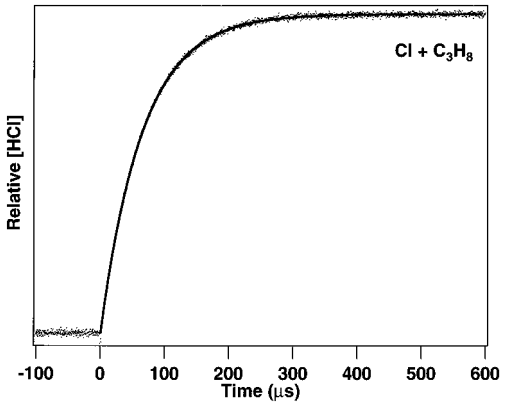

Figure 2. Typical absorption trace of the HCl reaction product vs time for the reaction Cl + propane → HCl + (*n,i*-)propyl. The solid line is a fit to a simple exponential rise (eq 1). The small spike at zero time is due to noise from the excimer photolysis laser thyratron. This trace is an average of 200 laser shots. Traces like this allow the pseudo-first order rate coefficient to be followed over at least four 1/e lifetimes.

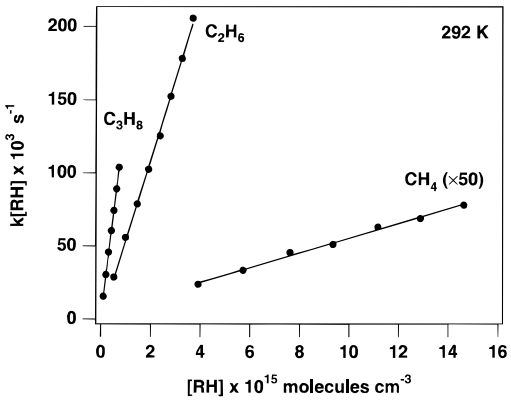

Figure 3. Typical plot of the measured pseudo-first-order rate coefficients vs alkane concentration for methane, ethane, and propane at room temperature (292 K). The rate coefficients for methane have been multiplied 50×.

found in all cases were less than 2% of the pseudo-first-order rate coefficients, indicating negligible background reactions.

At the higher temperatures of this study, thermal decomposition of the photolytic precursor is a potential problem. Photolytes that are attractive because of a large absorption cross section, such as CCl_4 and other halogenated methanes, may be undesirable because of their thermal instability.[18] On the other hand, several thermally stable photolytes such as CF_3Cl have small cross sections at 193 nm.[17] In these studies, CF_2Cl_2 is used almost exclusively because of its good thermal stability and reasonable cross section.[19] However, at the very highest temperatures, 700−800 K, where thermal decomposition may be a problem, CF_3Cl is used for comparison because of its exceptional thermal stability.[20]

Results

Methane. The reaction Cl + CH_4 → HCl + CH_3 is slightly endothermic with a $\Delta H°_{298}$ of +1.72 kcal mol^{-1}.[21] The second-order rate coefficient determined in this work at 292 K for Cl + CH_4 is 0.97(±0.1) × 10^{-13} cm^3 molecule^{-1} s^{-1}, where the error bounds are ±2σ precision only. This value is in good agreement with the accepted value of 1.0 × 10^{-13} cm^3 molecule^{-1} s^{-1} for the room temperature rate coefficient as given by the comprehensive reviews of Atkinson *et al.*[22] and DeMore *et al.*[23] In addition, a very recent study by Finlayson-Pitts and co-workers[24] using a fast flow discharge with resonance fluorescence detection gave a value of 0.94(± 0.04) × 10^{-13} cm^3 molecule^{-1} s^{-1}.

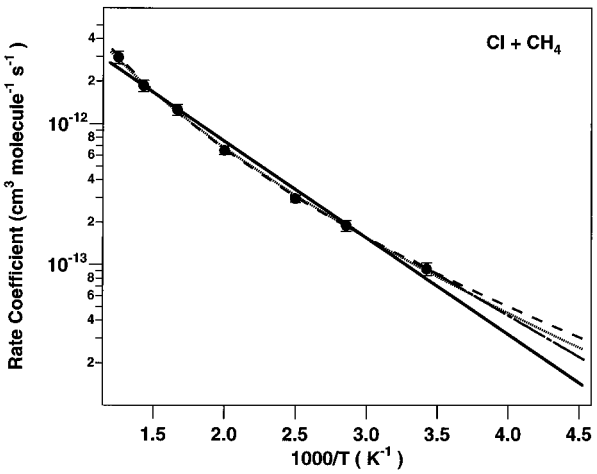

Figure 4. Semilogarithmic Arrhenius plot for the reaction Cl + CH_4. A fit using a simple Arrhenius expression, $k_{CH_4} = 1.8 \times 10^{-11} \exp(-1580/T)$ cm^3 molecule^{-1} s^{-1}, is given by the solid line. A modified Arrhenius fit, $k_{CH_4}(T) = [3.7(^{+8.2}_{-2.5}) \times 10^{-13}$ cm^3 molecule^{-1} s$^{-1}](T/298)^{2.6(\pm0.7)}$ $e^{-385(\pm320)/T}$, is given by the dashed line, and a fit with the temperature exponent held at 2, $k_{CH_4}(T) = 8.9(\pm0.9) \times 10^{-13}(T/298)^2$ $e^{-660(\pm40)/T}$, is given by the dotted line. The recommended value of Atkinson *et al*. is also shown as the dot−dash line for reference.[22] Error bars represent $\pm2\sigma$ precision only.

TABLE 1: Rate Coefficients for the Reactions Cl + Alkane → HCl + Alkyl[d]

temp (K)	k_{CH_4}[a]	$k_{C_2H_6}$[b]	$k_{C_3H_8}$[c]
292	0.93(9)	5.5(2)	1.38(2)
350	1.8(2)		1.38(5)
400	3.0(2)	6.0(3)	1.37(3)
450		6.4(1)	
500	6.5(4)	6.4(2)	1.37(1)
550		6.7(1)	
600	12.6(9)	7.0(3)	1.38(2)
650		7.1(1)	
700	18.6(9)	7.6(2)	1.38(3)
800	30(2)	8.1(7)	

[a] Units of 10^{-13} cm^3 molecule^{-1} s^{-1}. [b] Units of 10^{-11} cm^3 molecule^{-1} s^{-1}. [c] Units of 10^{-10} cm^3 molecule^{-1} s^{-1}. [d] The numbers in the parentheses indicate experimental uncertainties ($\pm$ 2σ precision only) in the last digit.

An Arrhenius plot for the Cl + methane reaction from 292 to 800 K is shown in Figure 4, and the rate data are shown in Table 1. A standard Arrhenius form can be fitted to the data, which is represented by the solid line in Figure 4. A simple Arrhenius fit to the temperature dependence of the rate coefficient, $k = A\ e^{-E_a/RT}$, gives

$$k_{CH_4} = [1.8(\pm0.6) \times 10^{-11}\ \text{cm}^3\ \text{molecule}^{-1}\ \text{s}^{-1}]\ e^{-1580(\pm150)/T} \quad (2)$$

where the $\pm2\sigma$ error limits represent the precision of the fit. This description for the rate coefficient reproduces the data over the temperature range investigated here to within 15% but falls outside the precision of the measurements. In order to adequately account for the temperature dependence, the data can be fit by a modified Arrhenius expression, $k = A'(T/298)^n\ e^{-E_a/RT}$. This yields

$$k_{CH_4}(T) = [3.7(^{+8.2}_{-2.5}) \times 10^{-13}\ \text{cm}^3\ \text{molecule}^{-1}\ \text{s}^{-1}](T/298)^{2.6(\pm0.7)}\ e^{-385(\pm320)/T} \quad (3)$$

where the temperature dependence of the pre-exponential factor is taken as an independent parameter. Error bars represent $\pm2\sigma$, precision only, assuming uncorrelated errors in the parameters. This parametrization of our rate coefficients fits the data to within experimental precision, with $\chi^2 = 3.6$, and is shown as the dashed line in Figure 4. However, the individual parameters are not very well characterized, and their uncertainties are strongly correlated. The data can also be fit to within our experimental errors ($\chi^2 = 6.7$) by an expression with n simply fixed at 2:

$$k_{CH_4}(T) = 8.9(\pm0.9) \times 10^{-13}(T/298)^2\ e^{-660(\pm40)/T} \quad (4)$$

represented by the dotted line in Figure 4. The recommended value of Atkinson *et al*. is also shown for reference.[22] The fit with $n = 2$ is more consistent with the thoroughly studied behavior of this reaction below room temperature, and extrapolations of both modified Arrhenius expressions, eqs 3 and 4, agree more closely with low-temperature rate data[25,26] than the simple Arrhenius expression, eq 2.

Although the reaction endothermicity and room temperature rate coefficient are well established, Ravishankara and Wine noted in temperature-dependent studies of this reaction, particularly below room temperature, a discrepancy in the measured rate coefficients depending on the kinetic method and initial reaction mixture conditions.[25] The discrepancy was postulated to be due to incomplete quenching of the excited spin−orbit state, $^2P_{1/2}$, for the Cl atom. In the present studies of the Cl + methane reaction, the concentration of the CF_2Cl_2 photolyte ($\sim3 \times 10^{14}$ molecules cm^{-3}) is sufficient to keep the quenching rate much faster than the primary reaction rate (quenching rate coefficient $\sim3.3(\pm 0.5) \times 10^{-10}$ cm^3 molecule^{-1} s^{-1}).[27] Thus, a true thermal distribution of spin−orbit states for Cl is maintained in these experiments. In addition, several measurements for all the alkanes have been performed using CF_3Cl as a photolyte. Because of the extremely small absorption cross section of CF_3Cl at 193 nm, up to 30% photolyte (densities of $\sim10^{17}$ cm^{-3}) is used in the reaction mixture to obtain acceptable signal levels. Assuming a quenching rate similar to that of CF_2Cl_2, the quenching rate at this concentration of CF_3Cl is at least 10^3 times faster than the reaction rate. Changing photolytes had no effect on the determined rate coefficients. Finally, Bersohn and co-workers[28] measured the branching fraction for production of Cl $^2P_{1/2}$ from CF_2Cl_2 at 193 nm. The excited spin−orbit state was found to contribute less than 5% of the Cl produced. Thus, nonthermal populations of excited-state chlorine atoms do not make a significant contribution to the overall rate coefficient in the present measurements.

There have been many previous investigations of the temperature dependence of this reaction. However, this study extends the high-temperature limit for an absolute rate determination. Whytock *et al.* obtained absolute rate coefficients from 299 to 500 K using the flash photolysis/resonance fluorescence technique.[29] They reported a value of $1.8(\pm0.28) \times 10^{-11}$ cm^3 molecule^{-1} s^{-1} for the pre-exponential factor, well within the error bars of the present determination. They determined the activation energy to be $E_a/R = 1545(\pm46)$ K, which is within the error bounds of the mean activation energy in the present study. In fact, most of the previous investigations that covered a temperature range similar to the one covered here obtain Arrhenius parameters similar to those of eq 2. Of these investigations, the highest temperature for which an absolute rate was measured is 686 K in the 1973 study of Clyne *et al.*[30] Although their pre-exponential was about a factor of 2 larger than in eq 2, the activation energy of $E_a/R = 1791(\pm36)$ K is only slightly outside our error bounds. Fits obtained in the lower temperature studies are reasonably accurate when extrapolated

to the higher temperatures of this investigation, with an extrapolation of the Arrhenius expression of Whytock *et al.* deviating by less than 20% from the measured value at 800 K. Nonetheless, the precision of our data clearly distinguishes the curvature in the Arrhenius plot over the temperature range 292−800 K.

The curvature in the Arrhenius plot for the Cl + CH_4 reaction is well-known and has been previously studied in some detail. The temperature dependence of this reaction has been studied between 200 and 500 K by Zahnizer *et al.*[26] who report the expression $k_{CH_4}(T) = 1.43 \times 10^{-12}(T/298)^{2.11} \exp(-795/T)$ cm^3 molecule^{-1} s^{-1}, which is in good agreement with the present measurements at higher temperatures. Whytock *et al.* reported a three-parameter fit to the rate coefficient over the temperature range 200−500 K, yielding $8.3 \times 10^{-13}(T/298)^{2.5} \exp(-608/T)$,[29] also in reasonable agreement with the present measurements. The temperature dependence of Cl + CH_4 was calculated by Heneghan *et al.* using thermodynamic transition-state theory (TST) methods.[31] Their estimate of the temperature-dependent rates is in qualitative agreement with the present results, although it significantly overpredicts the curvature (and hence the rate coefficient) above ∼500 K. The current study offers experimental measurements that can be used to validate calculations of the rate coefficient at higher temperatures.

Ethane. The Cl atom reaction with ethane can be expected to be faster than with methane because of the greater number of hydrogens and lower C−H bond strength in ethane (D_0 = 99.5 kcal mol^{-1} vs 103.3 kcal mol^{-1} for methane).[32] The Cl + ethane reaction is exothermic by ∼2.7 kcal mol^{-1} compared to the endothermic Cl + methane reaction.[21] The present determination gives $5.51(\pm0.22) \times 10^{-11}$ cm^3 molecule^{-1} s^{-1} for the room temperature rate coefficient. Since many relative rate studies have used this reaction as a reference, it becomes extremely important to measure this value as accurately as possible. As a result, there are many previous studies of this system. The reviews by Atkinson *et al.*[22] and DeMore *et al.*[23] approach a reasonable consensus from these studies for the room temperature rate coefficient. The rate recommended in the DeMore *et al.* review is $5.69(\pm0.60) \times 10^{-11}$ cm^3 molecule^{-1} s^{-1}. The value determined in the previous review of Atkinson *et al.* has been revised from this same value to $5.9(\pm0.9) \times 10^{-11}$ cm^3 molecule^{-1} s^{-1}. Both these values for the rate are somewhat higher than the present value. However, the error bars in the reviews easily encompass the present determination. More recently, Finlayson-Pitts and co-workers[24] report a value of $5.53(\pm0.21) \times 10^{-11}$ cm^3 molecule^{-1} s^{-1}, in good agreement with the present value. In addition, Lewis *et al.*[33] found the rate to be $5.48(\pm0.60) \times 10^{-11}$ cm^3 molecule^{-1} s^{-1}, which is again in agreement with the current value. Both these other determinations used the discharge flow/resonance fluorescence technique, while the present studies use the LP/IRLPA method. Previous investigations observed the loss of reactants, while we measure the appearance of products. It is encouraging that these different experimental approaches yield the same results. From the most recent studies and the present work, it seems clear that the room temperature rate is now well established and suggests a downward revision of the recommended value of Atkinson *et al.*[22]

The Arrhenius plot for Cl + ethane over the temperature range 292−800 K is shown in Figure 5 with the rate data given in Table 1. The data show marked deviation from linearity in the figure. Although the data are apparently linear with temperature at the lower region investigated, there is significant departure as the temperature increases. This departure appears more dramatic in this temperature range than in the methane data,

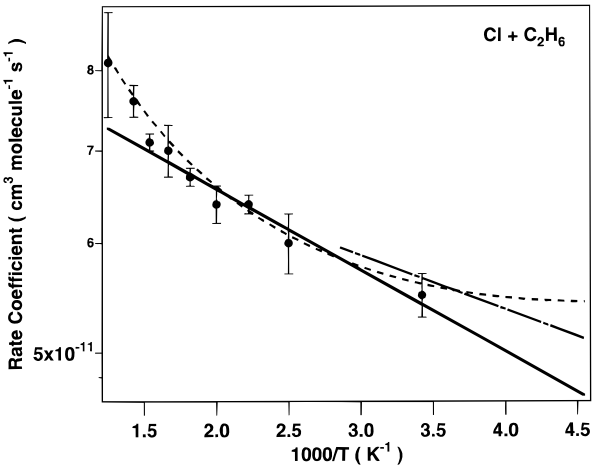

Figure 5. Semilogarithmic Arrhenius plot for the reaction Cl + ethane. There is marked deviation from linearity in the Cl + C_2H_6 reaction at temperatures above 600 K. The lower temperature data are fit to a simple Arrhenius expression (solid line). This fit yields an activation energy of E_a/R = 135 K and pre-exponential of 8.6×10^{-11} cm^3 molecule^{-1} s^{-1}. A modified Arrhenius fit $k_{C_2H_6}(T) = 3.4 \times 10^{-11}$ $(T/298)^{0.7}$ exp[150 /T] cm^3 molecule^{-1} s^{-1} is given by the dashed line. The recommended value of Atkinson *et al.* is also shown as the dot−dashed line for reference.[22] Error bars represent $\pm2\sigma$ precision only.

although the actual magnitude of the deviation is much smaller, and is most evident as the temperature increases above 600 K. Representation of our data by a modified Arrhenius expression,

$$k_{C_2H_6}(T) = [3.4(\pm1.4) \times 10^{-11} \text{ cm}^3 \text{ molecule}^{-1} \text{ s}^{-1}](T/298)^{0.7(\pm0.3)} e^{150(\pm110)/T} \quad (5)$$

gives the best fit to the experimental data. Error bars represent $\pm2\sigma$ precision only. This expression is given by the dotted line in Figure 5. At elevated temperatures the temperature dependence is dominated by that of the pre-exponential factor. The temperature dependence of the Cl + ethane pre-exponential factor is smaller than that for methane, based on the modified Arrhenius fits, but in the latter case the temperature dependence of the rate constant is dominated by the activation energy throughout the temperature region of this study.

The lower temperature (<600 K) data show little evidence of the curvature that is prominent in the higher temperature measurements. A simple Arrhenius expression can be fitted to the low-temperature data to facilitate comparison to previous investigations. This fit yields an Arrhenius expression of

$$k_{C_2H_6}(T) = [8.6(\pm 0.5) \times 10^{-11} \text{ cm}^3 \text{ molecule}^{-1} \text{ s}^{-1}]e^{-135(\pm26)/T} \quad (6)$$

where the error bars are $\pm2\sigma$. The fit is represented by the solid line in Figure 5. In the investigation of Lewis *et al.*[33] a pre-exponential factor of $9.01(\pm0.48) \times 10^{-11}$ cm^3 molecule^{-1} s^{-1} was obtained with an activation energy of $E_a/R = 133(\pm15)$ K. Their investigation employed the discharge flow/resonance fluorescence technique and spanned the temperature range 220−604 K. Clearly, our activation energy agrees well with theirs in this temperature range. Error bars on the respective pre-exponential factor determinations also bring both numbers into agreement. Another determination of this reaction rate coefficient is given in the study by Manning and Kurylo.[34] They employed the flash photolysis/resonance fluorescence technique from 222 to 322 K. Their pre-exponential factor was reasonably close to ours with a value of $7.3(\pm1.2) \times 10^{-11}$ cm^3 molecule^{-1} s^{-1}. Although agreement is poorer than with the Lewis study,

our combined error bars still overlap. However, their activation energy is only $E_a/R = 60(\pm 44)$ K, which is much lower than those of each of these other studies. It is possible that their limited temperature range was insufficient for an accurate determination. The Lewis study is the one most often cited for the absolute determination of these reaction parameters.

The two major review articles on this system by Atkinson *et al.* and DeMore *et al.* arrive at identical expressions for the temperature dependence. Their pre-exponential factor is 7.7×10^{-11} cm^3 molecule^{-1} s^{-1} with an activation energy of $E_a/R = 90$ K. This expression is valid over the temperature region 220−350 K. Both the pre-exponential and activation energy are slightly lower than those obtained in the present study. In fact the values lie slightly outside our error estimates. However, the respective temperature ranges barely overlap. In the Atkinson review the Arrhenius parameters are modified to $8.2(\pm 1.2) \times 10^{-11}$ cm^3 molecule^{-1} s^{-1} for the pre-exponential and $E_a/R = 100(\pm 100)$ K for the activation energy in the temperature range 220−600 K. This temperature range is comparable to that studied here, and the parameters are much closer to those obtained in the linear region of our Arrhenius plot. The modified Arrhenius expression, eq 5, which fits the present data, does not match the previously reported temperature dependence between 220 and 300 K. A reinvestigation of the temperature dependence in this region may be warranted.

The curvature in the Cl + ethane Arrhenius plot only becomes apparent when data above 600 K are included. We have undertaken a systematic analysis to determine whether this curvature could indicate the presence of experimental artifacts or could arise from contributions of new kinetic channels at high temperature. One obvious possible complication is thermal decomposition of the photolyte, which would generate Cl atoms independently of the photolysis laser and would also become increasingly important at higher temperature. However, this phenomenon would not have any direct relationship to the ethane concentration in the cell and, therefore, would not show up in the plot of pseudo-first-order rate coefficients vs [C_2H_6]. The reaction of this thermal source of Cl with ethane would result in a steady-state distribution of HCl across the cell and simply attenuate the IR beam. Thus, the rate should be independent of this complication. The reaction was also investigated using the more thermally stable photolyte, CF_3Cl, and the less stable CCl_4 precursor, and identical behavior was observed.

Another possibility is radical−radical recombination of the primary reaction products, whether formed by thermal or photolytic means. For example, the ethyl radicals produced in the reaction could combine to form *n*-butane, although the principal recombination products are ethane and ethylene. The *n*-butane would then react with the Cl atoms. Since the rate for Cl with *n*-butane is faster than that with ethane by about a factor of 4, this would lead to an increase in the apparent rate for the reaction. The rates obtained at room temperature and up to 600 K show no indication that this might be occurring. In fact, the recombination should be *less* important at higher temperature, since it is in essence an association reaction requiring collisional stabilization. However, production of ethyl radicals by reaction of thermolytically produced Cl atoms will increase at higher temperatures. But if this were a problem in the ethane system, it should be overwhelming in the methane system. The recombination of methyl radicals would result in the production of ethane, a molecule whose reaction with Cl atom is *500* times faster than that of the primary reactant. The same level of recombination products that would be necessary to produce the observed ∼12% deviation from linearity in the ethane system would increase the CH_4 measurement by almost a factor of 15. The rate coefficient for methyl radical recombination is faster than that for ethyl radical recombination, further increasing its relative importance. The absence of such an effect in the methane system is strong evidence that reaction with secondary or thermally produced products is unimportant in these measurements.

The increased rate coefficient cannot be attributed to reaction with the photolyte, leftover reaction products, or impurities in the either the reagent or buffer gases. Reaction with the photolyte or products formed in the previous reaction pulse would only result in a nonzero intercept in the plots of pseudo-first-order rate coefficients vs [RH], since they do not depend on the concentration of the primary reactant. In any case, the photolyte concentration was varied over a factor of 5 without measurable difference in the rate coefficient. Alternatively, an unknown impurity in the primary reactant gas could explain a higher reaction coefficient. However, the impurity must be extremely reactive to chlorine but also have a steep temperature dependence for reaction; otherwise, the effect would be evident at all temperatures, not just above 600 K. The hydrocarbon impurities in the 99.97% ethane (100 ppm propylene, 200 ppm propane) are not consistent with such behavior.

Since the possible sources of error are not capable of explaining the nonlinear Arrhenius behavior in the Cl + ethane reaction, we consider whether new kinetic phenomena could be responsible for the deviation. One possible explanation is that a new reaction channel opens up between the Cl atom and ethane at the increased temperatures. The only other available channel in this reaction is the breaking of the carbon−carbon bond in ethane. The two possible product pathways for this bond fission are to $CH_3Cl + CH_3$, with $\Delta H°_{298}$ of +6.4 kcal mol^{-1} and to $CH_2Cl + CH_4$, with $\Delta H°_{298}$ of +2.4 kcal mol^{-1}.[21] In order to account for the observed behavior in the Arrhenius plot, the high-temperature process must have an activation energy of ∼5.2 kcal mol^{-1} and a pre-exponential factor of $\sim 3.5 \times 10^{-10}$ cm^3 molecule^{-1} s^{-1}. Such an activation energy could be accommodated by an endothermic reaction channel, such as that to $CH_2Cl + CH_4$. However, it seems implausible that the pre-exponential factor for the bond fission process is the near-gas kinetic value needed to explain the Cl + C_2H_6 temperature dependence.[35] End product analysis, especially at higher temperatures, could rule out or confirm carbon−carbon bond fission. Although the contribution of a competing bond fission channel cannot be definitely excluded, it seems highly unlikely.

The spin−orbit splitting, ΔE, between the $^2P_{3/2}$ ground state (Cl) and the $^2P_{1/2}$ excited state (Cl*) is 882 cm^{-1} or $\Delta E/k = 1269$ K. Consequently, there will be an appreciable thermal population in the excited state at the higher temperatures of this study. For example, at 800 K approximately 10% of the Cl atoms are in the excited spin−orbit state. The excited spin−orbit state does not correlate adiabatically with ground-state products, so curve crossing to the ground-state surface is required for reaction. A higher rate coefficient for Cl* than for Cl with CH_4 has been postulated based on the low-temperature studies of Ravishankara and Wine.[25] This hypothesis was rationalized by assuming that the electronic energy in the Cl* becomes available for overcoming the activation energy in the Cl + CH_4 reaction. For ethane, the activation barrier is minimal, so the energetic effect on the reaction may be different.

Fitting the observed ethane temperature dependence by reaction of thermal Cl* requires values of $\sim 8 \times 10^{-10}$ cm^3 molecule^{-1} s^{-1} and ∼1200 K for the pre-exponential and E_a/R, respectively. If the electronic energy transfer limits the reaction, the activation energy for Cl* reaction may simply reflect the barrier to curve crossing. An activation energy of $E_a/R = 1200$

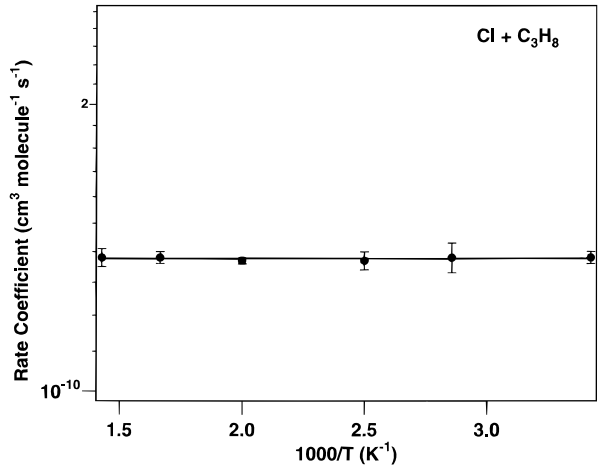

Figure 6. Temperature dependence of the Cl + propane reaction. The rate coefficient is 1.38(± 0.3) × 10^{-10} cm^3 $molecule^{-1}$ s^{-1} between 292 and 700 K.

K is reasonable in such a situation. The pre-exponential factor, however, is unusually large, a factor of 3 or 4 greater than a normal gas kinetic collision rate. Cross sections for electronic quenching can be rather large, but it is doubtful that a pre-exponential of such a size can be accommodated by Cl* electronic energy transfer. For comparison, the rate coefficient for Cl [$^2P_{1/2}$] removal by an efficient quencher such as CF_2Cl_2 is only ∼3.3(± 0.5) × 10^{-10} cm^3 $molecule^{-1}$ s^{-1}.[27] The contribution of the reaction with Cl* must be considered at higher temperatures but is unlikely to be responsible for the curvature in the Cl + ethane Arrhenius plot.

The temperature dependence of the pre-exponential factor in the Cl + C_2H_6 reaction is smaller than that for Cl + CH_4. The temperature dependence in the methane reaction is qualitatively described by transition-state theory calculations. Detailed calculations of the Cl + ethane reaction as a function of temperature would be extremely valuable for determining whether the observed temperature dependence can be described by a temperature-dependent transition state for primary hydrogen abstraction.[36] Hydrogen abstraction reactions from ethane by other radicals, e.g., by CN[37] or OH,[38] show a T^n behavior for primary hydrogen abstraction with n typically between 1 and 2. However, the more exothermic abstraction of secondary hydrogens by CN, which shows a $T^{0.5}$ dependence,[37] appears more similar to the Cl + ethane reaction. The present measurements extend to the range where shock-tube techniques can be applied. Higher temperature data for Cl + ethane, in addition to a reinvestigation of the rate coefficients below 300 K, would be valuable for further characterizing this reaction.

Propane. For the reaction of Cl with propane there are two distinct pathways for reaction, one resulting in formation of the *n*-propyl radical and the other in formation of the isopropyl radical. The present experiment does not discriminate between these two pathways, and the rate coefficients obtained are the sum of the two. Primary hydrogen abstraction to yield *n*-propyl and HCl is 2 kcal mol^{-1} exothermic at 298 K, and secondary hydrogen abstraction to yield isopropyl and HCl is 4.8 kcal mol^{-1} exothermic at 298 K.[21] The enhanced exothermicity for the secondary hydrogen abstraction simply reflects the greater stability of a secondary carbon radical relative to a primary. The measured rate coefficient for Cl + C_3H_8 is 1.38(±0.02) × 10^{-10} cm^3 $molecule^{-1}$ s^{-1} at 292 K. The rate coefficient was not found to change with temperature over the range 292−700 K as shown by the rate data in Table 1 and in Figure 6. The rate coefficient over the entire temperature range is given by 1.38(± 0.03) × 10^{-10} cm^3 $molecule^{-1}$ s^{-1}.

There have been relatively few studies of the Cl + propane reaction. Of these few, three obtained values for the room temperature rate coefficient only.[24,39,40] These values range from 1.3 × 10^{-10} to 1.6 × 10^{-10} cm^3 $molecule^{-1}$ s^{-1}. Our room temperature rate coefficient falls within this range. The most recent study is that of Finlayson-Pitts and co-workers[24] using the fast flow discharge technique. They obtained a reaction rate of 1.23(±0.10) × 10^{-10} cm^3 $molecule^{-1}$ s^{-1} at 298 K. The review of Atkinson *et al.*[22] recommends a value of 1.4(±0.4) × 10^{-10} cm^3 $molecule^{-1}$ s^{-1}, while the recommendation of DeMore *et al.*[23] is 1.6(±0.6) × 10^{-10} cm^3 $molecule^{-1}$ s^{-1}. Our value is lower than the recommended value of DeMore *et al.* but in reasonable agreement with the rate given in the fast flow discharge determination. Additionally, the value determined in our LP/IRLPA method is in excellent agreement with that in the review of Atkinson *et al.* These more recent determinations support the lower value recommended by Atkinson *et al*.

There have been only two studies of the temperature dependence in this system. The first was a relative rate study in 1955 by Pritchard *et al.*[1] They report a negative activation energy of $E_a/R = -337(\pm 100)$ K between 298 and 484 K. The only other study was in 1980 by Lewis *et al.*[33] using a discharge flow/resonance fluorescence technique. Absolute rate coefficients were obtained in the Lewis study at three temperatures over the 220−607 K temperature range. In their study, they reported a negative activation energy of $E_a/R = -44(\pm 50)$ K. However, recognizing the limited data set, they gave an alternative description of the rate as just the mean of the determined rates. Currently accepted values for this reaction rate coefficient as given by the reviews of DeMore *et al.* and Atkinson *et al.* have reported the negative activation energy of Lewis *et al.* In the present study, a larger temperature range spanning 400 K was covered and no indication of a negative temperature dependence was found. The present study establishes the Cl + propane reaction to be independent of temperature between 292 and 700 K.

Conclusions

Rate coefficients for the reaction of Cl atom with methane and ethane have been measured between 292 and 800 K and with propane between 292 and 700 K. The reaction with methane shows significant curvature on an Arrhenius plot, confirming earlier transition-state theory calculations. The reaction with ethane displays a marked deviation from simple Arrhenius behavior above 600 K, which can be modeled using a $T^{0.7\pm0.3}$ dependence of the pre-exponential. The reaction with propane is independent of temperature over the range of these experiments. Further work, especially shock-tube studies, would be valuable for improving the understanding of the Cl + C_2H_6 reaction at high temperatures.

Acknowledgment. The authors thank Richard Jennings for his expert technical assistance in the development of the experimental apparatus. This work is supported by the Division of Chemical Sciences, Office of Basic Energy Sciences, U.S. Department of Energy.

References and Notes

(1) Pritchard, H. O.; Pyke, J. B.; Trotman-Dickenson, A. F. *J. Am. Chem. Soc.* **1955**, *77*, 2629.

(2) Kaiser, E. W.; Rimai, L.; Schwab, E.; Lim, E. C. *J. Phys. Chem.* **1992**, *96*, 303.

(3) Chiltz, G.; Eckling, R.; Goldfinger, P.; Huybrechts, G.; Johnson, H. S.; Meyers, L.; Verbeke, G. *J. Chem. Phys.* **1963**, *38*, 1053.

(4) Dobis, O.; Benson, S. W. *J. Am. Chem. Soc.* **1991**, *113*, 6377.

(5) Atkinson, R.; Aschmann, S. M. *Int. J. Chem. Kinet.* **1987**, *19*, 1097.

(6) Wallington, T. J.; Andino, J. M.; Lorkovic, I. M.; Kaiser, E. W.; Marston, G. *J. Phys. Chem.* **1990**, *94*, 3644.
(7) Wallington, T. J.; Kaiser, E. W. *J. Phys. Chem.* **1996**, *100*, 4111.
(8) Petek, H.; Nesbitt, D. J.; Ogilby, P. R.; Moore, C. B. *J. Phys. Chem.* **1983**, *87*, 5367.
(9) Yan, Y.-B; Hall, J. L.; Stephens, J. W.; Richnow, M. L.; Curl, R. F. *J. Chem. Phys.* **1987**, *86*, 1657.
(10) Schiffman, A.; Nelson, D. D., Jr.; Robinson, M. S.; Nesbitt, D. J. *J. Phys. Chem.* **1991**, *95*, 2629.
(11) Pine, A. S. *J. Opt. Soc. Am.* **1976**, *66*, 97.
(12) Herriott, D.; Kogelnik, H.; Kompfner, R. *Appl. Opt.* **1964**, *3*, 523. Herriott, D. R.; Schulte, H. J. *Appl. Opt.* **1965**, *4*, 883.
(13) Trutna, W. R.; Byer, R. L. *Appl. Opt.* **1980**, *19*, 301.
(14) Pilgrim, J. S.; Jennings, R. T.; Taatjes, C. A. *Rev. Sci. Instrum.*, in press.
(15) Yardley, J. T. *Introduction to Molecular Energy Transfer*; Academic: New York, 1980.
(16) Taatjes, C. A.; Leone, S. R. *J. Chem. Phys*. **1988**, *89*, 302.
(17) Okabe, H. *Photochemistry of Small Molecules*; John Wiley & Sons: New York, 1978; pp 305−306.
(18) Michael, J. V.; Lim, K. P.; Kumaran, S. S.; Kiefer, J. H. *J. Phys. Chem.* **1993**, *97*, 1914.
(19) Kumaran, S. S.; Lim, K. P.; Michael, J. V.; Wagner, A. F. *J. Phys. Chem.* **1995**, *99*, 8673.
(20) Kiefer, J. H.; Sathyanarayana, R.; Lim, K. P.; Michael, J. V. *J. Phys. Chem.* **1994**, *98*, 12278.
(21) Lide, D. R. *Handbook of Chemistry and Physics*, 76th ed.; CRC Press: Boca Raton, FL, 1995; Chapters 5 and 9.
(22) Atkinson, R.; Baulch, D. L.; Cox, R. A.; Hampson, R. F., Jr.; Kerr, J. A.; Troe, J. *J. Phys. Chem. Ref. Data* **1992**, *21*, 1416.
(23) De More, W. B.; Sander, S. P.; Golden, D. M.; Hampson, R. F.; Kurylo, M. J.; Howard, C. J.; Ravishankara, A. R.; Kolb, C. E.; Molina, M. J. Chemical Kinetics and Photochemical Data for use in Stratospheric Modeling. Evaluation No. 10, JPL Publication, 92-20; Jet Propulsion Laboratory: Pasadena, CA, 1992.
(24) Beichert, P; Wingen, L.; Lee, J.; Vogt, R.; Ezell, M. J.; Ragains, M.; Neavyn, R.; Finlayson-Pitts, B. J. *J. Phys. Chem.* **1995**, *99*, 13156.
(25) Ravishankara, A. R.; Wine, P. H. *J. Chem. Phys.* **1980**, *72*, 25.
(26) Zahniser, M. S.; Berquist, B. M.; Kaufman, F. *Int. J. Chem. Kinet.* **1978**, *10*, 15.
(27) Tyndall, G. S.; Orlando, J. J.; Kegley-Owen, C. S. *J. Chem. Soc., Faraday Trans.* **1995**, *91*, 3055.
(28) Matsumi, Y.; Tonokura, K.; Kawasaki, M.; Inoue, G.; Satyapal, S.; Bersohn, R. *J. Chem. Phys.* **1991**, *94*, 2669.
(29) Whytock, D. A.; Lee, J. H.; Michael, J. V.; Payne, W. A.; Stief, L. J. *J. Chem. Phys.* **1977**, *66*, 2690.
(30) Clyne, M. A. A.; Walker, R. F. *J. Chem. Soc., Faraday Trans.* **1973**, *69*, 1547.
(31) Heneghan, S. P.; Knoot, P. A.; Benson, S. W. *Int. J. Chem. Kinet.* **1981**, *13*, 677.
(32) Berkowitz, J.; Ellison, G. B.; Gutman, D. *J. Phys. Chem.* **1994**, *98*, 2744.
(33) Lewis, R. S.; Sander, S. P.; Wagner, S.; Watson, R. T. *J. Phys. Chem.* **1980**, *84*, 2009.
(34) Manning, R. G.; Kurylo, M. J. *J. Phys. Chem.* **1977**, *81*, 291.
(35) Benson, S. W. *Thermochemical Kinetics*; John Wiley & Sons: New York, 1976.
(36) Hu, X; Hase, W. L. *J. Phys. Chem.* **1989**, *93*, 6029.
(37) Hess, W. P.; Durant, J. L.; Tully, F. P. *J. Phys. Chem.* **1989**, *93*, 6402.
(38) Atkinson, R. Kinetics and Mechanisms of the Gas-Phase Reactions of the Hydroxyl Radical with Organic Compounds. *J. Phys. Chem. Ref. Data, Monogr*. **1989**, *1*.
(39) Atkinson, R.; Aschmann, S. M. *Int. J. Chem. Kinet.* **1985**, *17*, 33.
(40) Wallington, T. J.; Skewes, L. M.; Siegl, W. O.; Wu, C.-H.; Japar, S. M. *Int. J. Chem. Kinet.* **1988**, *20*, 867.